

## Research Article

# *In Silico* Study of *Leishmania donovani* $\alpha$ - $\beta$ Tubulin and Inhibitors

Tamiris M. Assis, Daiana T. Mancini, Teodorico C. Ramalho, and Elaine F. F. da Cunha

Departamento de Química, Universidade Federal de Lavras, Caixa Postal 3037, 37200-000 Lavras, MG, Brazil

Correspondence should be addressed to Teodorico C. Ramalho; teo@dqf.ufla.br

Received 14 February 2014; Accepted 28 April 2014; Published 1 July 2014

Academic Editor: Hugo Verli

Copyright © 2014 Tamiris M. Assis et al. This is an open access article distributed under the Creative Commons Attribution License, which permits unrestricted use, distribution, and reproduction in any medium, provided the original work is properly cited.

*Leishmania donovani* is a parasite that causes visceral leishmaniasis, a severe form of leishmaniasis that affects vital organs. An important target for the treatment of this disease is the protein  $\alpha$ - $\beta$  tubulin, which was modeled in this paper and proposed as a target for the treatment of visceral leishmaniasis. Two classes of compounds were studied, dinitroanilines and oxadiazoles. According to the docking results, dinitroanilines interact better with the L loop domain and oxadiazoles interact better with the colchicine domain.

## 1. Introduction

Protozoan infections are diseases that affect hundreds of millions of people worldwide. In this scenario, leishmaniasis is a neglected disease caused by protozoan parasites of the genus *Leishmania*. There are at least 20 species of this genus that give rise to different types of manifestations, ranging from cutaneous injuries to visceral leishmaniasis or Kalazar [1, 2]. The visceral leishmaniasis is the most severe form, because the parasite *Leishmania donovani* usually migrates to vital organs such as liver, spleen, and bone marrow. The parasite exists in two forms, the mobile promastigotes form, found in the intestine of the female vector, the Sandfly, and the amastigote form, found in the mammalian host, which is the cause of the disease [3]. The pentavalent antimonials are the drugs of first choice for treatment of Kalazar, but they have high toxicity, limited effectiveness, and intolerance [4]. The drugs most used in the treatment of the disease are meglumine antimoniate (Glucantime) and sodium stibogluconate (pentosan), but they are injectables [5]. Currently, an orally administered drug, miltefosine, is known; however, it has teratogenic effects and high cost [4]. Microtubules are crucial to cell division and intracellular organelle transport, hence, recognized as an important target for therapy for several diseases [6]. They are made of repeated  $\alpha$ - $\beta$  tubulin heterodimers, which are associated in parallel forming a wall

of microtubules, giving rise to the polymer [7]. Existing drugs used as microtubule inhibitors have high toxicity and their use is limited because of resistance [8]. Therefore, there is need for discovery of new drugs superior to the existing.

In this work, the three-dimensional structure of the *Leishmania donovani*  $\alpha$ - $\beta$  tubulin (LdTUB) was built by homology modeling and then applied in molecular docking techniques to study the interaction mode of dinitroaniline and 1,2,4-oxadiazole inhibitors of this protein. The molecular details of the interaction of these inhibitors with the LdTUB are quite unknown. Probably dinitroaniline interacts with the N loop alpha subunit [9] and 1,2,4-oxadiazole interacts with the colchicine domain [10].

## 2. Experimental

**2.1. Homology Modeling.** The modeling began with the systematic search in the database ExPasy [11] for primary structures of the protein  $\alpha$ - $\beta$  tubulin in LdTUB using the server Protein Knowledgebase (UniProtKB) [12] as a search tool. Thus, we obtained the primary alpha (Q25262\_LEIDO, 451 amino acids) and beta (I3W8N7\_LEIDO, 442 amino acids) sequences. The crystal structure of pig tubulin heterodimer (protein data bank code: ITUB) was chosen as the template for the construction of the three-dimensional LdTUB model, as it showed the highest sequence identity therewith [13].

Once the template was chosen, the primary sequence of the target protein was aligned with the template protein using the LALIGN server. The model was constructed on a SWISS-MODEL server and the Swiss-Pdb Viewer program [14, 15]. A trimer was constructed in order to analyze the potential binding sites of the protein.

For validation, we used the program PROCHECK [18, 19], which assesses the stereochemical quality of protein structures and the root mean square deviation (RMSD), which superimposes the structures of proteins and calculates the deviation.

**2.2. Inhibitors Studied.** Were studied two classes of tubulin inhibitors, described by Bhattacharya et al. [16] (Table 1, Compounds 1–11) and Cottrell et al. [17] (Table 1, Compounds 12–18), which are shown in Table 1. The biological activities of these compounds were reported as a negative logarithm of the concentration capable of inhibiting 50% of the tubulin activity ( $PIC_{50} = -\log IC_{50}$ ).

**2.3. Molecular Docking.** The three-dimensional structure of each inhibitor was built using the program PC Spartan Pro [20] and its partial charges were calculated by the semiempirical PM3 method. The compounds were docked into the protein LdTUB using Molegro Virtual Docker (MVD) software [21, 22]. The binding site was limited to a sphere with a 9 Å radius. The MVD allows determining the most probable conformation between protein and ligand by estimating the interaction energy. The best poses are those that have lower energy. The function values used in the anchoring (Docking Scoring Function) are defined by the following equation:

$$E_{\text{score}} = E_{\text{inter}} + E_{\text{intra}}, \quad (1)$$

where

$$E_{\text{inter}} = \sum_{i \in \text{ligand}} \sum_{j \in \text{protein}} \left[ E_{\text{PLP}}(r_{ij}) + 332.0 \frac{q_i q_j}{4r_{ij}^2} \right]. \quad (2)$$

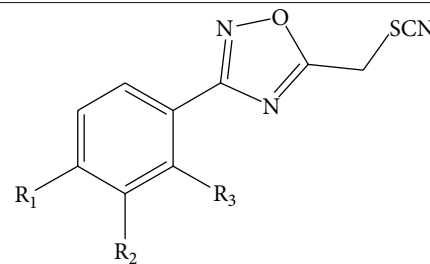
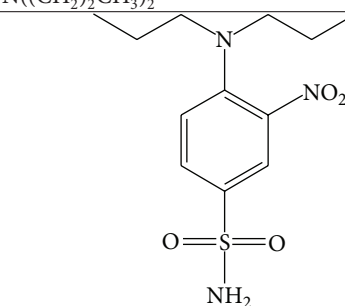
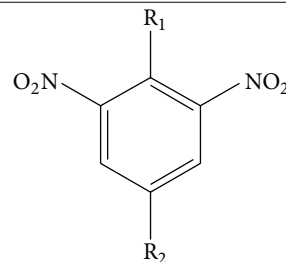
The term  $E_{\text{PLP}}$  highlights the ‘‘piecewise linear potential,’’ which uses two different sets of parameters as follows: one for approximation to the steric term (van der Waals) between the atoms and the other potential for hydrogen bonding. The second term describes the electrostatic interactions between overloaded atoms. It is a Coulomb potential with a dielectric constant which depends on the distance ( $D(r) = 4r$ ).  $E_{\text{intra}}$  is the internal energy of the ligand:

$$E_{\text{intra}} = \sum_{i \in \text{ligand}} \sum_{j \in \text{ligand}} E_{\text{PLP}}(r_{ij}) + \sum_{\text{flexible bonds}} A [1 - \cos(m \cdot \theta - \theta_0)] + E_{\text{clash}}. \quad (3)$$

The first term (double sum) is between all pairs of atoms in the ligand excluding atom pairs that are connected by two bridges. The second term is a torsional energy term, where  $\theta$  is the angle of twist ties. The average contribution of the torsion link is used if several torsions are determined. The last term  $E_{\text{clash}}$  assigns a penalty of 1000 if the distance between two heavy atoms (more than two separate titles) is less than 2.0 Å.

TABLE 1: Compounds synthesized by Bhattacharya et al. [16] and Cottrell et al. [17].

Compound	R <sub>1</sub>	R <sub>2</sub>	R <sub>3</sub>
1-ORYZALIN	N((CH <sub>2</sub> ) <sub>2</sub> CH <sub>3</sub> ) <sub>2</sub>	SO <sub>2</sub> NH <sub>2</sub>	
2	pyrrolidino	SO <sub>2</sub> NH <sub>2</sub>	
3	N((CH <sub>2</sub> ) <sub>2</sub> CH <sub>3</sub> ) <sub>2</sub>	CONH <sub>2</sub>	
4	N(CH <sub>2</sub> CH <sub>3</sub> ) <sub>2</sub>	SO <sub>2</sub> NH <sub>2</sub>	
5	NH(CH <sub>2</sub> ) <sub>2</sub> CH <sub>3</sub>	SO <sub>2</sub> NH <sub>2</sub>	
6	N((CH <sub>2</sub> ) <sub>3</sub> CH <sub>3</sub> ) <sub>2</sub>	SO <sub>2</sub> NH <sub>2</sub>	
7	N((CH <sub>2</sub> ) <sub>2</sub> CH <sub>3</sub> ) <sub>2</sub>	C <sub>6</sub> H <sub>5</sub>	
8	N((CH <sub>2</sub> ) <sub>5</sub> CH <sub>3</sub> ) <sub>2</sub>	SO <sub>2</sub> NH <sub>2</sub>	
9	N((CH <sub>2</sub> ) <sub>4</sub> CH <sub>3</sub> ) <sub>2</sub>	SO <sub>2</sub> NH <sub>2</sub>	
10	N((CH <sub>2</sub> ) <sub>2</sub> CH <sub>3</sub> ) <sub>2</sub>	CN	
11			
12	H	H	Cl
13	H	H	H
14	OCH <sub>3</sub>	H	H
15	H	H	Cl
16	CH <sub>3</sub>	H	H
17	F	H	H
18	Cl	H	H
19	Cl	Cl	H



	10	20	30	40	50	60
Ld	MREAI	CIHIGQAGCQVGNACWELFCLEHGIQPDGSMPSDKCIGVEDDAFN	TFSETGAGK			
	10	20	30	40	50	60
1TUB	MRECISIHVGQAGVQIGNACWELYCLEHGIQPDGQMP	SDKTIGGGDDSFNTFFSETGAGK				
	70	80	90	100	110	120
Ld	HVPRCIFLDLEPTVVDEVRTGTYRQLFNPEQLVSGKEDAANN	YARGHYTIGKEIVDLALD				
	70	80	90	100	110	120
1TUB	HVPRAVFDLEPTVIDEVRTGTYRQLFHPEQLITGKEDAANN	YARGHYTIGKEIDLVL				
	130	140	150	160	170	180
Ld	RIRKLADNCTGLQGFMVFHAVGGTGSGLGALLERLSVDY	GKSKLGYTVYSPQVSTA				
	130	140	150	160	170	180
1TUB	RIRKLADQCTGLQGFVSFHSFGGTSGFTSLLMERLSVDY	GKSKLEFSIYPAPQVSTA				
	190	200	210	220	230	240
Ld	VVEPYNVCLSTHSLLEHTDVATMLDNEAIYDLTRRSLDIER	PSYTNVNR	LIGQVSSLTA			
	190	200	210	220	230	240
1TUB	VVEPYNVCLSTHSLLEHTDVATMLDNEAIYDLTRRSLDIER	PTYNLNR	LIGQVSSITA			
	250	260	270	280	290	300
Ld	SLRFDGALNVDLTEFQTNLVPYPRIHVFLTSYAPVVS	AEKAYHEQLSVADITNSVFEPAG				
	250	260	270	280	290	300
1TUB	SLRFDGALNVDLTEFQTNLVPYPRAHFPLATYAPVISA	EKAYHEQLSVAEITNACFEPAN				
	310	320	330	340	350	360
Ld	MLTKCDPRHGKYMCCCLMYRGDVVPKDVNAAIATIKTKR	TIQFVDWCPTGFKCGINYP				
	310	320	330	340	350	360
1TUB	QMVKCDPRHGKYMCCCLLYRGDVVPKDVNAAIATIKTKR	TIQFVDWCPTGFKVGINYEP				
	370	380	390	400	410	420
Ld	TVVPGDLAKVQRAVCMIANSTAEVFAEIDHKFDL	MYSKRAVHVHVVYVGE	MEEGEFSE			
	370	380	390	400	410	420
1TUB	TVVPGDLAKVQRAVCMISNTTAEAWARLDHKFDL	MYAKRAVHVHVVYVGE	MEEGEFSE			
	430	440	450			
Ld	AREDLAAVEKDYEEVGAESADDMGEEDVEEY					
	430	440	450			
1TUB	AREDMAALEKDYEEVGVDSVEGEGEEEGEEY					

FIGURE 1: Alignment of alpha subunits. Key: single letters: amino acids. “.”: identical. “.”: conserved substitutions.

### 3. Results and Discussion

**3.1. Homology Modeling.** In the first stage of this work, the primary sequence of the 1TUB dimer was aligned with the sequence of the LdTUB dimer using the LALIGN server. The alignments (Figures 1 and 2) showed that  $\alpha$  and  $\beta$  proteins have 85.0% and 79% sequence identity, respectively. These values suggest that 1TUB and LdTUB may share a similar overall structure. According to Ceslovas Venclovas, only if the aligned sequences are over 40–50% identical to

each other and have few or no gaps can it be expected that alignments may be accurate in a structural sense [23]. Thus, the alignment was considered satisfactory for modeling the LdTUB tridimensional structure. SWISS-MODEL was used to generate the  $\alpha$  and  $\beta$  models and the Maestro (Maestro, version 9.0, Schrödinger, LLC, New York, NY, 2009) program was used for energy minimization with the consistent valence force field (OPLS) until the maximum derivative  $1.0 \text{ kcal mol}^{-1}$ . After that, the alpha-beta-alpha trimer was constructed and energy was minimized.

```

          10      20      30      40      50      60
Ld      MREAICIHIGQAGCQVGNACWELFCLEHGIQPDGSMPSDKCIGVEDDAFNITFFSETGAGK
      : : : : : : : : : : : : : : : : : : : : : : : : : : : : : : : : : : : :
1TUB    MRECISIHVGQAGVQIGNACWELYCLEHGIQPDGQMPSDKTIGGGDDSFNITFFSETGAGK
          10      20      30      40      50      60

          70      80      90      100     110     120
Ld      HVPRCIFLDLEPTVVDEVRTGTYRQLFNPEQLVSGKEDAANNYARGHYTIGKEIVDLALD
      : : : : : : : : : : : : : : : : : : : : : : : : : : : : : : : : : : : :
1TUB    HVPRAVFDLEPTVIDEVRTGTYRQLFHPEQLITGKEDAANNYARGHYTIGKEIIDLVLD
          70      80      90      100     110     120

          130     140     150     160     170     180
Ld      MREIVSCQAGQCGNQIGSKFWEVIADEHGVDPTGSYQGDSDLQLERINVYFDESTGGRYV
      : : : : : : : : : : : : : : : : : : : : : : : : : : : : : : : : : : : :
1TUB    MREIVHIQAGQCGNQIGAKFWEVISDEHGIDPTGSYHGSDLQLERINVYNEAAGNKYV
          130     140     150     160     170     180

          190     200     210     220     230     240
Ld      PRAVLMDELEPGTMDSVRAGPYQLFRPDNFIFGQSGAGNNWAKGHYTEGAELIDSVLDVC
      : : : : : : : : : : : : : : : : : : : : : : : : : : : : : : : : : : : :
1TUB    PRAILVDLEPGTMDSVRSGPFGQIFRPDNFVFGQSGAGNNWAKGHYTEGAELVDSVLDVV
          190     200     210     220     230     240

          250     260     270     280     290     300
Ld      RKEAESCDCLQGFQLSHSLGGGTGSGMGTLLISKLREEYPDRIMMTFVSPRVSVDTVV
      : : : : : : : : : : : : : : : : : : : : : : : : : : : : : : : : : : : :
1TUB    RKESESCDCLQGFQLTHSLGGGTGSGMGTLLISKIREEYPDRIMMNTFSVVPSPKVSVDTVV
          250     260     270     280     290     300

          310     320     330     340     350     360
Ld      EPYNTLSVHQLVENDESMECIDNEALYDICFRTLKLTPTFGDLNHLVAAMVSGVTCCCL
      : : : : : : : : : : : : : : : : : : : : : : : : : : : : : : : : : : : :
1TUB    EPYNATLSVHQLVENTDETYCIDNEALYDICFRTLKLTPTYGDLNHLVSATMSGVTTCCL
          310     320     330     340     350     360

          370     380     390     400     410     420
Ld      RFPGQLNSDLRKLAVNLVPPFRLHFFMMGSAPLTSRGSQQYRGLSVAELTQQMFDAKNMM
      : : : : : : : : : : : : : : : : : : : : : : : : : : : : : : : : : : : :
1TUB    RFPGQLNADLRKLAVNMVPPFRLHFFMPGFAPLTSRGSQQYRALTVPELTQQMFDAKNMM
          370     380     390     400     410     420

          430     440     450     460     470     480
Ld      QAADPRHGRYLTASALFRGRMSTKEVDEQMLNVQKNSSYFIEWIPNNIKSSICDIPPKG
      : : : : : : : : : : : : : : : : : : : : : : : : : : : : : : : : : : : :
1TUB    AACDPRHGRYLTVAAVFRGRMSMKEVDEQMLNVQKNSSYFVEWIPNNVKTAVCDIPPRG
          430     440     450     460     470     480

          490     500     510     520     530     540
Ld      LKMSVTFIGNNTCIQEMFRRVGEQFTGMFRKAFLHWYTGEGMDEMEFTEAESNMNDLVS
      : : : : : : : : : : : : : : : : : : : : : : : : : : : : : : : : : : : :
1TUB    LKMSATFIGNSTAIQELFKRISEQFTAMFRKAFLHWYTGEGMDEMEFTEAESNMNDLVS
          490     500     510     520     530     540

          550
Ld      EYQQYQDATVEEGEYEEEE
      : : : : : : : : : : : : : : : : : : : : : : : : : : : : : : : : : : : :
1TUB    EYQQYQDATADEQGEFEEEE
          550

```

FIGURE 2: Alignment of beta subunits. Key: single letters: amino acids. “.”: identical. “?”: conserved substitutions.

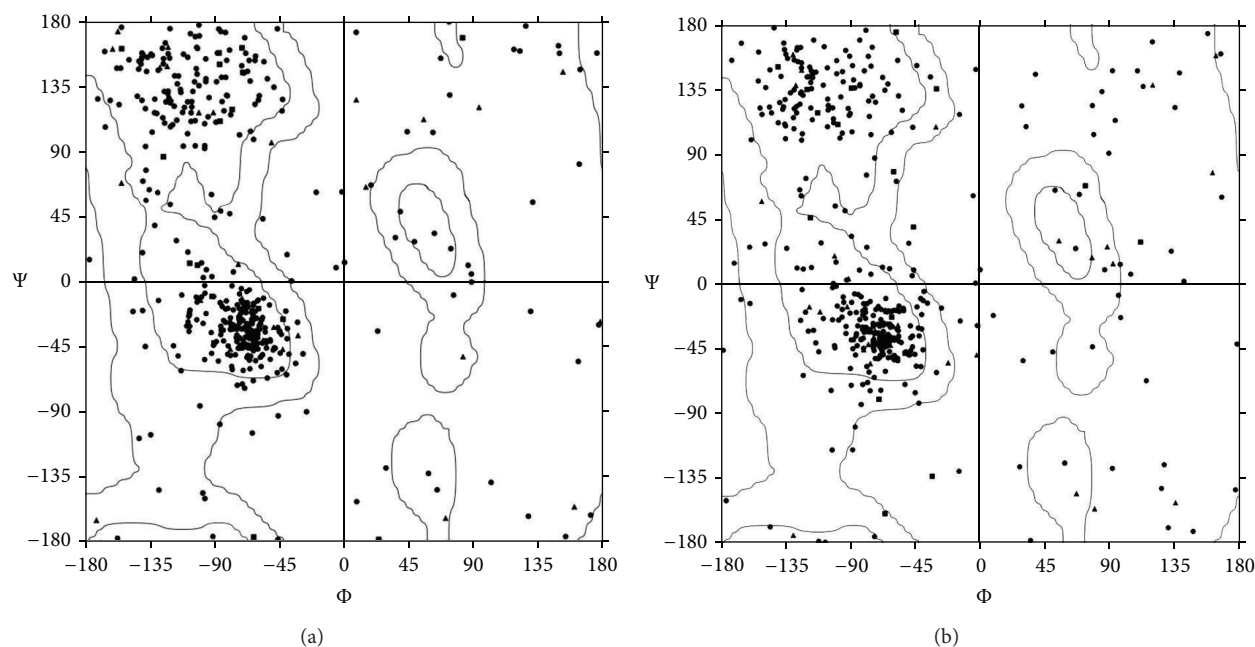


FIGURE 3: Ramachandran plot for the alpha subunit (a) and beta subunit (b).

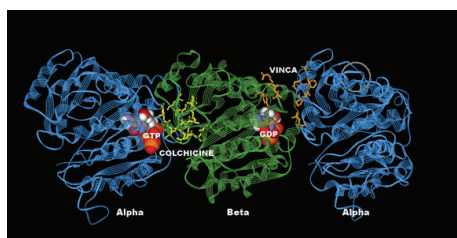


FIGURE 4: Three-dimensional model of LdTUB. The colchicine and vinca domains are shown in yellow and orange, respectively. L loop is shown with circle.

**3.2. Model Validation.** Validation is an essential step that can be implemented at different levels of structural organization. One should evaluate the overall quality of the packing of the protein and the possible errors in structural parameters. The Ramachandran plot (Figures 3 and 4) obtained with the PROCHECK program showed that, in alpha and beta subunits, respectively: (i) 74.4% and 66.5% of the residues are in the most favored regions; (ii) 15.7% and 20.0% of the residues are in additional allowed regions; (iii) 5.7% and 7.0% are of the residues are in generously allowed regions; (iv) 4.2% and 6.5% of the residues in disallowed regions. It can be concluded that LdTUB model is of good quality and is energetically favored and stable. Some amino acid residues are found in disallowed regions; however, it was found that these residues are not part of any protein domain, so it was not necessary to perform any calculations to fit these residues in more detail. The superimposing between the template backbone and target enzymes was available using the Swiss-Pdb Viewer 3.7 program [14, 15].

Superimposed tertiary structures of proteins' (backbone) mold and target found RMSD (root-mean-square deviation) of 0.26 and 0.34 Å for alpha and beta, respectively. It is known from the literature that RMSD values of 0.7 Å are found in identical proteins in different crystal forms, and values in the order of 2 Å are found in homologous proteins with 30% identity [24–27]. Figure 4 shows the 3D LdTUB structure proposed by homology modeling utilizing ITUB. GDP and GTP cofactors that were added to the model and the complex were slowly relaxed to clean the starting structure.

**3.3. Dinitroaniline and Oxadiazole Binding Sites.** The colchicine binding sites of LdTUB were calculated and a cavity was observed close to Ile367 $\beta$ , Thr365 $\beta$ , Ile352 $\beta$ , Ser351 $\beta$ , Ser350 $\beta$ , Lys349 $\beta$ , Ile348 $\beta$ , Asn347 $\beta$ , Asn346 $\beta$ , Phe316 $\beta$ , Leu315 $\beta$ , Ala314 $\beta$ , Ser313 $\beta$ , Ala312 $\beta$ , Thr311 $\beta$ , Leu256 $\beta$ , Asn355 $\beta$ , Val354 $\beta$ , Ala353 $\beta$ , Leu352 $\beta$ , Lys351 $\beta$ , Arg250 $\beta$ , Leu249 $\beta$ , Asp248 $\beta$ , Ser247 $\beta$ , Asn246 $\beta$ , Leu245 $\beta$ , Arg240 $\beta$ , Leu239 $\beta$ , Thr236 $\beta$ , Val235 $\beta$ , Fly234 $\beta$ , Val181 $\alpha$ , Ala180 $\alpha$ , Thr179 $\alpha$ , Ser178 $\alpha$ , Ala143 $\alpha$ , and Asn101 $\alpha$ . The vinca binding sites of LdTUB were observed close to Ile355 $\alpha$ , Gly354 $\alpha$ , Cys353 $\alpha$ , Lys352 $\alpha$ , Phe351 $\alpha$ , Gly350 $\alpha$ , Thr349 $\alpha$ , Lys336 $\alpha$ , Ala333 $\alpha$ , Ile332 $\alpha$ , Ala331 $\alpha$ , Ala330 $\alpha$ , Asn329 $\alpha$ , Val328 $\alpha$ , Lys326 $\alpha$ , Pro325 $\alpha$ , Tyr319 $\alpha$ , Leu317 $\alpha$ , Leu248 $\alpha$ , Ala247 $\alpha$ , Leu224 $\beta$ , Pge221 $\beta$ , Thr220 $\beta$ , Pro219 $\beta$ , Tyr207 $\beta$ , Glu204 $\beta$ , Asn203 $\beta$ , Asp176 $\beta$ , Ser175 $\beta$ , Val174 $\beta$ , and Arg173 $\beta$ . Morrisette et al. analyzed oryzalin (Table 1, Compound 1) resistance in *T. gondii* [28]. They demonstrated that dinitroanilines bind to  $\alpha$ -tubulin. The site identified is located beneath the N loop and is composed of Arg2 $\alpha$ , Glu3  $\alpha$ , Val4 $\alpha$ , Trp21 $\alpha$ , Phe24 $\alpha$ , His28 $\alpha$ , Ile42 $\alpha$ , Asp47 $\alpha$ , His61, Pro63, Arg64 $\alpha$ , Cys65 $\alpha$ , Cys129, Thr239 $\alpha$ , Arg243 $\alpha$ , and Phe244 $\alpha$  residues. Thus, this region was also studied and named N loop domain.

TABLE 2: Activity of dinitroaniline analogues against leishmanial tubulin *in vitro* and energy values (kcal mol<sup>-1</sup>) for docked pose.

Compd	% inhibition of LdTUB	Colchicine domain $E_{\text{Score}}$	Vinca domain $E_{\text{score}}$	L loop domain $E_{\text{Score}}$
1	54.0	-100.4	-97.9	-105.8
2	57.0	-98.4	-119.6	-109.4
3	34.0	-98.3	-113.9	-97.7
4	58.0	-97.5	-116.3	-109.0
5	43.0	-99.5	-122.7	-90.5
6	89.0	-94.8	-129.5	-119.9
7	108.0	-101.0	-138.6	-129.6
8	48.0	-117.6	-63.8	-118.6
9	95.0	-114.1	-142.3	-122.6
10	25.0	-103.7	-108.0	-71.9
11	19.0	-92.9	-93.3	-81.7

TABLE 3: Antiparasitic activities of oxadiazole analogues against *L. donovani in vitro* and energy values (kcal mol<sup>-1</sup>) for docked pose.

Compd	pIC <sub>50</sub>	Colchicine domain $E_{\text{Score}}$	Vinca domain $E_{\text{Score}}$	N loop domain $E_{\text{Score}}$
12	57.0	-90.25	-93.3	-6.89
13	19.0	-92.16	-88.78	-67.65
14	34.0	-97.78	-85.36	-67.92
15	58.0	-99.19	-95.91	-71.69
16	43.0	-111.43	-90.73	-97.71
17	54.0	-110.16	-98	-56.70
18	89.0	-108.24	-96.87	-70.45
19	108.0	-115.61	-99.48	-49.73

3.4. *Docking Studies.* Energy score values were calculated to get a better understanding of the differences between the binding modes of each compound in known sites of the tubulin protein and the factors that affect its activity. This procedure was performed for the two classes of compounds studied and similar compounds.

Table 2 presents the experimental values of the inhibition % of leishmanial tubulin assembly at 20 mM dinitroaniline analogues and estimated energy score (MolDockScore) between inhibitor and enzyme obtained with the docking in each tubulin domain. The theoretical results obtained in molecular docking were compared with the experimental results described by the Bhattacharya et al. [16]. Linear regression was used to model the relationship between the independent energy term values and inhibition values by fitting a linear equation to the observed data. The theoretical results obtained by the docking study of the dinitroaniline analogs with colchicine and vinca domains were not well correlated ( $r_{\text{colchicine}}^2 = 0.04$  and  $r_{\text{vinca}}^2 = 0.42$ ) with the experimental results. However, the results obtained by the docking of the dinitroaniline analogs with N loop domain were correlated ( $r_{\text{Nloop}}^2 = 0.78$ ). Thus, the experimental values agree better with theoretical values from N loop domain results than with the vinca and colchicine. By analyzing the hydrogen bond formed between the eleven compounds (1–11) and the LdTUB active site, we observed (i) compounds 1, 5, 9, and 11 exhibited hydrogen bonds with Ser38; (ii) Compounds 1–4, 6, and 7 interacted with Ile42; (iii) Compounds 1 and 5–7 interacted with His28; (iv) Compounds 1, 2, 4, 6, 7, and

11 interacted with Leu26; (v) Compounds 4 and 7 interacted with Phe24; (vi) Compounds 1, 5, 6, and 9 interacted with Lys40; (vii) all compounds interacted with Cys25. It is evident from Table 2 that Compound 7 interacts more strongly with L loop domain than other compounds. That compound is the most potent because the substituent at the N1 position of the sulfanilamide core is bulkier (Figure 5). Through the docking results, it was observed that the ring at position R2 is directed to Asp39 of the active site, interacting through  $\pi$  interaction.

Table 3 presents the experimental values of the antileishmanial pIC<sub>50</sub> and estimated energy between inhibitor and enzyme obtained with the docking in each tubulin domain. The theoretical results obtained in the molecular docking were compared with the experimental results described by Cottrel et al. [17]. Similarly to dinitroaniline inhibitors, linear regression was used for energy term and inhibition value relationships by fitting a linear equation to the observed data. The theoretical results obtained by the docking study of the oxadiazole analogs with N loop and vinca domain were not well correlated ( $r_{\text{Nloop}}^2 = 0.06$  and  $r_{\text{vinca}}^2 = 0.43$ ) with the experimental results. However, the results obtained by the docking of the oxadiazole analogs with colchicine domain were correlated ( $r_{\text{colchicine}}^2 = 0.80$ ). This suggests that the experimental values agree better with theoretical values from colchicine domain results than with the vinca and N loop. By analyzing the hydrogen bond formed between the eight compounds (12–18) and the LdTUB active site, we observed (i) Compounds 12, 15, and 18 exhibited hydrogen

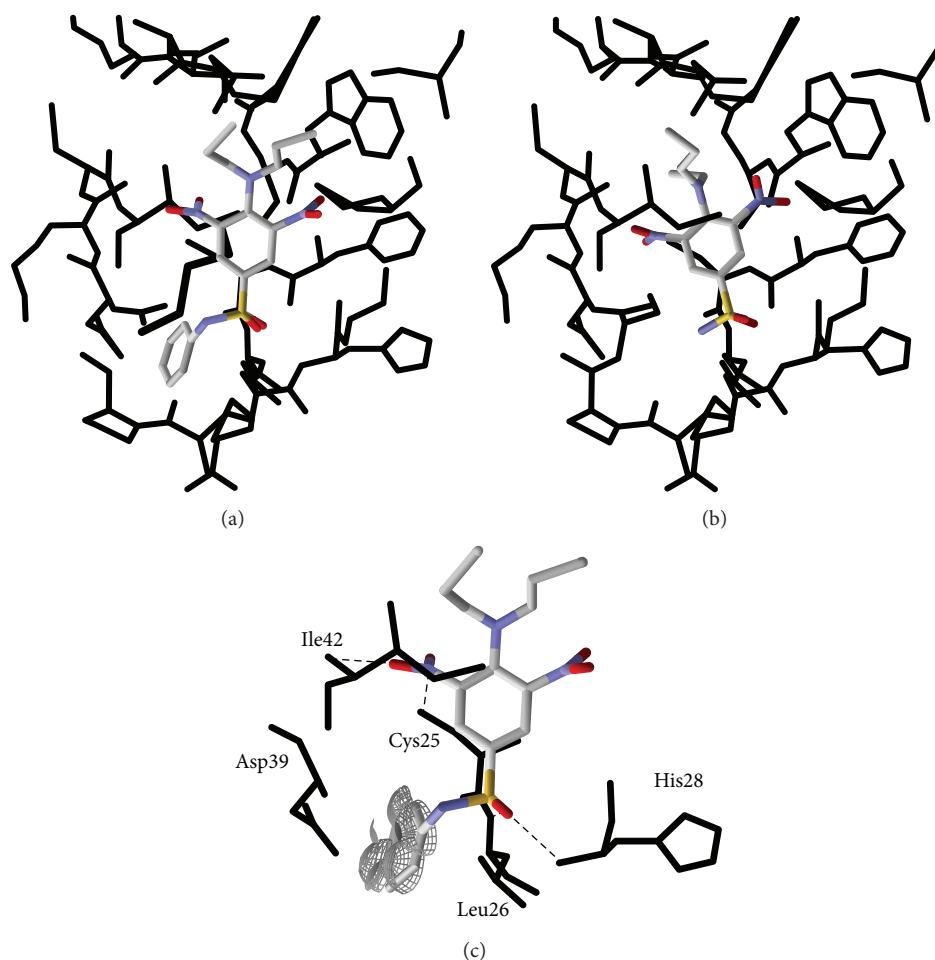


FIGURE 5: (a) Compound 7 inside L loop domain. (b) Oryxalin inside L loop domain. (c) Electrostatic interactions between the Compound 7 and L loop are shown with dashed line (hydrogen bonds) and half sphere.

bonds with Lys251 $\beta$ ; (ii) Compounds 12, 13, 14, 16, and 17 interacted with Lys359 $\beta$ ; (iii) all compounds interacted with Ser257 $\beta$ . The SCN group of compounds 12–18 is directed to GTP (electrostatic interaction). The more potent oxadiazole is 18 (Table 3). It is the only compound with two substituent groups in the ring.

#### 4. Conclusion

In the present work, the LdTUB active site binding mode interactions of dinitroaniline and oxadiazole analogs were studied. According to the docking results, dinitroanilines interact better with L loop domain and the aromatic ring at the N1 position should be explored. Oxadiazoles interact better with the colchicine domain and those analogs with two substituents in the aromatic ring should be explored.

#### Conflict of Interests

The authors declare that there is no conflict of interests regarding the publication of this paper.

#### Acknowledgments

The authors thank the Brazilian agencies FAPEMIG, CAPES, and CNPq for funding part of this work.

#### References

- [1] S. Bhowmick and N. Ali, "Identification of novel *Leishmania donovani* antigens that help define correlates of vaccine-mediated protection in visceral leishmaniasis," *PLoS ONE*, vol. 4, no. 6, Article ID e5820, 2009.
- [2] J. Kaur, R. Tiwari, A. Kumar, and N. Singh, "Bioinformatic analysis of *Leishmania donovani* long-chain fatty acid-CoA ligase as a novel drug target," *Molecular Biology International*, vol. 2011, Article ID 278051, 14 pages, 2011.
- [3] M. J. A. Queiroz, J. G. B. Alves, and J. B. Correia, "Visceral leishmaniasis: clinical and epidemiological features of children in an endemic area," *Jornal de Pediatria*, vol. 80, no. 2, pp. 141–146, 2004.
- [4] T. S. Tiuman, A. O. Santos, T. Ueda-Nakamura, B. P. D. Filho, and C. V. Nakamura, "Recent advances in leishmaniasis treatment," *International Journal of Infectious Diseases*, vol. 15, no. 8, pp. e525–e532, 2011.

- [5] R. K. Kar, M. Y. Ansari, P. Suryadevara et al., "Computational elucidation of structural basis for ligand binding with *Leishmania donovani* adenosine kinase," *BioMed Research International*, vol. 2013, Article ID 609289, 14 pages, 2013.
- [6] L. Luis, M. L. Serrano, M. Hidalgo, and A. Mendoza-León, "Comparative analyses of the  $\beta$ -tubulin gene and molecular modeling reveal molecular insight into the colchicine resistance in kinetoplastids organisms," *BioMed Research International*, vol. 2013, Article ID 843748, 8 pages, 2013.
- [7] K. L. Schaefer, "PPAR- $\gamma$  inhibitors as novel tubulin-targeting agents," *Expert Opinion on Investigational Drugs*, vol. 16, no. 7, pp. 923–926, 2007.
- [8] C. Y. Nien, Y. C. Chen, C. C. Kuo et al., "5-Amino-2-Aroylquinolines as highly potent tubulin polymerization inhibitors," *Journal of Medicinal Chemistry*, vol. 53, no. 5, pp. 2309–2313, 2010.
- [9] C. Ma, C. Li, L. Ganesan et al., "Mutations in  $\alpha$ -tubulin confer dinitroaniline resistance at a cost to microtubule function," *Molecular Biology of the Cell*, vol. 18, no. 12, pp. 4711–4720, 2007.
- [10] A. Kamal, A. Viswanath, M. J. Ramaiah et al., "Synthesis of tetrazole-isoxazoline hybrids as a new class of tubulin polymerization inhibitors," *Medicinal Chemistry Communications*, vol. 3, no. 11, pp. 1386–1392, 2012.
- [11] <http://au.expasy.org/>.
- [12] R. Apweiler, "The universal protein resource (UniProt)," *Nucleic Acids Research*, vol. 36, no. 1, pp. D190–D195, 2008.
- [13] M. Goodarzi, E. F. F. da Cunha, M. P. Freitas, and T. C. Ramalho, "QSAR and docking studies of novel antileishmanial diaryl sulfides and sulfonamides," *European Journal of Medicinal Chemistry*, vol. 45, no. 11, pp. 4879–4889, 2010.
- [14] K. Arnold, L. Bordoli, J. Kopp, and T. Schwede, "The SWISS-MODEL workspace: a web-based environment for protein structure homology modelling," *Bioinformatics*, vol. 22, no. 2, pp. 195–201, 2006.
- [15] F. Kiefer, K. Arnold, M. Künzli, L. Bordoli, and T. Schwede, "The SWISS-MODEL repository and associated resources," *Nucleic Acids Research*, vol. 37, supplement 1, pp. D387–D392, 2009.
- [16] G. Bhattacharya, M. M. Salem, and K. A. Werbovetz, "Antileishmanial dinitroaniline sulfonamides with activity against parasite tubulin," *Bioorganic and Medicinal Chemistry Letters*, vol. 12, no. 17, pp. 2395–2398, 2002.
- [17] D. M. Cottrell, J. Capers, M. M. Salem, K. DeLuca-Fradley, S. L. Croft, and K. A. Werbovetz, "Antikinetoplastid activity of 3-aryl-5-thiocyanatomethyl-1,2,4-oxadiazoles," *Bioorganic and Medicinal Chemistry*, vol. 12, no. 11, pp. 2815–2824, 2004.
- [18] R. A. Laskowski, M. W. MacArthur, D. S. Moss, and J. M. Thornton, "PROCHECK: a program to check the stereochemical quality of protein structures," *Journal of Applied Crystallography*, vol. 26, pp. 283–291, 1993.
- [19] R. A. Laskowski, J. A. C. Rullmann, M. W. MacArthur, R. Kaptein, and J. M. Thornton, "AQUA and PROCHECK-NMR: programs for checking the quality of protein structures solved by NMR," *Journal of Biomolecular NMR*, vol. 8, no. 4, pp. 477–486, 1996.
- [20] W. J. Hehre, *A Guide to Molecular Mechanics and Quantum Chemical Calculations*, Wavefunction, Inc., Irvine, Calif, USA, 2003.
- [21] M. C. Guimarães, D. G. Silva, E. G. da Mota, E. F. F. da Cunha, and M. P. Freitas, "Computer-assisted design of dual-target anti-HIV-1 compounds," *Medicinal Chemistry Research*, vol. 23, no. 3, pp. 1548–1558, 2014.
- [22] E. F. F. da Cunha, J. E. Resende, T. C. C. Franca et al., "Molecular modeling studies of piperidine derivatives as new acetylcholinesterase inhibitors against neurodegenerative diseases," *Journal of Chemistry*, vol. 2013, Article ID 278742, 7 pages, 2013.
- [23] A. J. Orry and R. Abagyan, "Homology modeling: methods and protocols," in *Methods in Molecular Biology*, vol. 857, Springer Science+Business Media, LLC, 2012.
- [24] D. Josa, E. F. F. da Cunha, T. C. Ramalho, T. C. S. Souza, and M. S. Caetano, "Homology modeling of wild-type, D516V, and H526L *Mycobacterium tuberculosis* RNA polymerase and their molecular docking study with inhibitors," *Journal of Biomolecular Structure & Dynamics*, vol. 25, no. 4, pp. 373–376, 2008.
- [25] A. P. Guimarães, A. A. Oliveira, E. F. F. da Cunha, T. C. Ramalho, and T. C. C. França, "Design of new chemotherapeutics against the deadly anthrax disease. Docking and molecular dynamics studies of inhibitors containing pyrrolidine and riboamidrazone rings on nucleoside hydrolase from *Bacillus anthracis*," *Journal of Biomolecular Structure and Dynamics*, vol. 28, no. 4, pp. 455–469, 2011.
- [26] E. J. Barreiro, C. A. M. Fraga, A. L. P. Miranda, and C. R. Rodrigues, "A química medicinal de N-acilidrazonas: novos compostos-protótipos de fármacos analgésicos, antiinflamatórios e anti-trombóticos," *Química Nova*, vol. 25, pp. 129–148, 2002.
- [27] O. A. Santos Filho and R. B. de Alencastro, "Modelagem de proteínas por homologia," *Química Nova*, vol. 26, no. 2, pp. 253–259, 2003.
- [28] N. S. Morrisette, A. Mitra, D. Sept, and L. D. Sibley, "Dinitroanilines bind  $\alpha$ -tubulin to disrupt microtubules," *Molecular Biology of the Cell*, vol. 15, no. 4, pp. 1960–1968, 2004.





**Hindawi**

Submit your manuscripts at  
<http://www.hindawi.com>

